

band<sup>10</sup> upon excitation by ultraviolet showed that the quantum efficiency *increased* as the incident photon flux increased for excitation by 7.7-eV photons. For excitation with photons having an energy of 5.7 eV the quantum efficiency was independent of the incident photon intensity. It is noted that 5.7 eV is just less than the band gap of NaI (5.8 eV)<sup>20</sup> while a 7.7-eV photon is capable of producing ionizing events. As the excitation intensity with 7.7-eV photons increases, the steady-state density of I<sub>2</sub><sup>-</sup> ions increases while the density of other electron traps (associated with impurities or imperfections) remains constant. On the basis of the present interpretation this situation would lead to an increase in the quantum efficiency of the ultraviolet band as the excitation intensity increases, in accord

<sup>20</sup> J. E. Eby, K. J. Teegarden, and D. B. Dutton, Phys. Rev. **116**, 1099 (1959).

with experiment. The fact that the ultraviolet emission band is stimulated by light in the fundamental band region (5.7 eV and below in NaI) indicates that the ultraviolet band may result from the radiative decay of an exciton, as previously suggested by Van Sciver.<sup>11</sup> This implies that the excited state of both the (I<sub>2</sub><sup>-</sup>+e) center and the exciton decay radiatively with the same emission spectrum. The interpretation suggested in this paper is, therefore, similar to that previously given by Van Sciver<sup>11</sup> with regard to the emitting excited state.

#### ACKNOWLEDGMENTS

The authors are indebted to J. H. Crawford, Jr., and A. Meyer of this Laboratory, and to F. E. Williams, University of Delaware, for helpful discussions and comments.

## Helicons and Magnons in Magnetically Ordered Conductors

EDWARD A. STERN\*

*University of Maryland, College Park, Maryland*

AND

EARL R. CALLEN†

*U. S. Naval Ordnance Laboratory, White Oak, Silver Spring, Maryland and Department of Physics, Catholic University, Washington, D. C.*

(Received 13 March 1963)

The character of magnons and helicons in magnetically ordered conductors is considered. Conductors become transparent to circularly polarized electromagnetic waves, helicons, when  $\omega_c\tau \gg 1$ , where  $\omega_c$  is the cyclotron frequency and  $\tau$  is the relaxation time of the conduction electrons. It is shown that, in general, there exists a strong coupling between helicons and magnons, so strong that a perturbative approach is not adequate. The effect of this strong coupling is calculated and is shown to produce large effects on the magnon and helicon spectra at long wavelengths. The coupling between magnons and helicons can be varied by changing the external magnetic field. These effects should be experimentally observable.

WE consider the problem of the existence of helicons in magnetically ordered conductors, and their interaction with spin waves. A helicon, called a whistler in atmospheric physics, is a mode of propagation of a circularly polarized electromagnetic wave through a charged plasma in a magnetic field. Recently, helicons have been observed in very pure metals at liquid-helium temperatures<sup>1-3</sup> where they have also been called magnetoplasma oscillations. In the limit approached in these experiments of  $\omega_c\tau \gg 1$ , where  $\omega_c$  is the cyclotron

frequency of the electrons in the magnetic field and  $\tau$  is their relaxation time, the electron plasma is transparent to one sense of circularly polarized radiation, the one that rotates in the same direction as the electrons around the magnetic field, while it is reflecting to the other sense. The angular frequency,  $\omega$ , of the helicons of wave number  $q$  is given by the usual relation for electromagnetic waves

$$\omega^2 = (c^2/\mu\epsilon)q^2, \quad (1)$$

where  $\mu$  and  $\epsilon$  are the magnetic permeability and dielectric constants, respectively. For nonmagnetic metals and for frequencies near zero<sup>2</sup>

$$\epsilon = 4\pi nec/\omega B, \quad (2)$$

and to a good approximation  $\mu = 1$ . Here  $B$  is the magnetic induction and there are  $n$  effective conduction

\* Supported in part by the Advanced Research Projects Agency.

† Supported in part by the Office of Naval Research.

<sup>1</sup> R. Bowers, C. Legency, and F. Rose, Phys. Rev. Letters **7**, 339 (1961); F. Rose, M. Taylor, and R. Bowers, Phys. Rev. **127**, 1122 (1962).

<sup>2</sup> R. G. Chambers and B. K. Jones, Proc. Roy. Soc. (London) **A270**, 417 (1962).

<sup>3</sup> P. Cotti, P. Wyder, and A. Quattronani, Phys. Letters **1**, 50 (1962).

electrons per unit volume of charge  $e$ . The net density being given by the difference between the electron and hole densities.

The ratio of the magnetic field and the electric field  $E$  of the helicon is given by

$$B/E = (\epsilon\mu)^{1/2},$$

which for nonmagnetic metals is equal to about  $10^{11}/\sqrt{\omega}$ . The frequency  $\omega$  is always much less than  $\omega_c \approx 10^{11}$  so that it is seen that the helicons are practically all magnetic field.

### I. HELICONS IN MAGNETIC CONDUCTORS

In the case of magnetically ordered conductors, the situation for the propagation of helicons is more complicated. Not only must the conduction electrons be considered, but, in addition, the ordered spins of the system are strongly coupled to the magnetic field of the helicons and their effects must be included. Furthermore, the spin-orbit interaction of the conduction electrons can be important for magnetically ordered materials. Before any detailed models are considered, we will derive a general expression for the interaction of spin waves with the helicons.

For simplicity, we consider the case of a single-crystal, single-domain ferro- or ferrimagnet, with the external field and the magnetization lying along an easy axis and a spin wave propagating along the magnetization direction; for other directions of propagation the analysis is complicated by the tensor nature of  $\mu$  and  $\epsilon$  but no new physics occurs. As the spins precess they produce a time-varying magnetic induction field  $B$  which induces currents in the conductor. These currents produce a magnetic field which acts back on the spins. The induced currents are a forced helicon mode and are the coupling mechanism between helicons and magnons. We can also see this coupling by starting with a transverse helicon propagating along the magnetization direction. The magnetic field of the helicons will tilt the spins away from the magnetization direction. This displacement of the spins rotates around with the magnetic field of the helicon and induces a forced spin-wave motion.

We calculate this coupling between magnons and helicons by use of Maxwell's equations. We shall ignore all surface effects, such as surface currents and magnetostatic modes, thereby limiting the applicability of our treatment to wavelengths short compared with the sample size. Assume that a transverse magnon varying in time and space as  $\exp[i(qz - \omega t)]$  is propagating along the  $z$  direction which is also the easy magnetization and external magnetic field directions. The circularly polarized time-varying component of the magnetization,  $M_\phi$ , is in the  $x$ - $y$  plane and is given by

$$\mathbf{M}_\phi = m(\mathbf{i} + i\mathbf{j}) \exp[i(qz - \omega t)], \quad (3)$$

where  $\mathbf{i}$  and  $\mathbf{j}$  are unit vectors in the  $x$  and  $y$  directions, respectively. From Maxwell's equations

$$q^2 \mathbf{H}_\phi = (\omega^2 \epsilon / c^2) (\mathbf{H}_\phi + 4\pi \mathbf{M}_\phi). \quad (4)$$

Here  $\mathbf{H}_\phi$  is the induced magnetic field produced by the conduction electrons and  $\epsilon$  is the dielectric constant of the solid, which is considered, in general, to be complex to include all conductivity effects. Equation (4) is easily solved for  $\mathbf{H}_\phi$  giving

$$\mathbf{H}_\phi = 4\pi \mathbf{M}_\phi (q^2 c^2 / \omega^2 \epsilon - 1)^{-1}. \quad (5)$$

Neglecting phenomenological damping effects, the motion of the spins is determined by<sup>4</sup>

$$d\mathbf{M}_\phi/dt = \gamma(\mathbf{M} \times \mathbf{H}) + (\alpha/M_s) \mathbf{M} \times \nabla^2 \mathbf{M}, \quad (6)$$

where

$$\mathbf{H} = \mathbf{H}_m + \mathbf{H}_\phi$$

and

$$\mathbf{H}_m = \mathbf{H}_{\text{anis}} + \mathbf{H}_0. \quad (7)$$

Here  $M_s$  is the saturation magnetization,  $\mathbf{H}_{\text{anis}}$  is the magnetic anisotropy field,  $\mathbf{H}_0$  is the external field, and  $\gamma = ge/2mc$ . The second term on the right-hand side of (6) is due to the exchange interaction between the oriented spins. The solution of (6) gives

$$\omega = \omega_m - 4\pi M_s \gamma (q^2 c^2 / \omega^2 \epsilon - 1)^{-1}, \quad (8)$$

where

$$\omega_m = \gamma H_m + \alpha q^2,$$

the magnon spectrum if there were no coupling to helicons.

Expression (8) can be rewritten, in a more transparent fashion so that it has the form of Eq. (1), in which case we find that

$$\mu = 1 + \gamma 4\pi M_s / (\omega_m - \omega). \quad (8')$$

The general relationship given in (8) has already been derived in various forms for different problems.<sup>5-8</sup> In these previous cases the high-conductivity limit,  $\omega_c \tau \gg 1$ , where helicons exist, was not considered. We will consider this limit.

### II. FREE-ELECTRON GAS

Consider the model of a degenerate free-electron gas imbedded in a uniform positively charged background so that there is macroscopic charge neutrality. As shown later in this section  $\epsilon$  is generally a function of

<sup>4</sup> L. Landau and E. Lifshitz, *Physik. Z. Sowjetunion* **8**, 153 (1935).

<sup>5</sup> W. S. Ament and G. T. Rado, *Phys. Rev.* **97**, 1558 (1955).

<sup>6</sup> C. Kittel, *Phys. Rev.* **110**, 840 (1958).

<sup>7</sup> B. A. Auld, *J. Appl. Phys.* **31**, 1642 (1960). Auld has considered the case of a magnetic insulator with a frequency and wave number-independent dielectric constant. Two branches also appear analogous to the two branches described in this paper. However, the dependence of frequency on wave number is different. The low-frequency branch begins linearly with wave number instead of the square of the wave number and the upper branch has no upper limit instead of approaching a constant frequency as in this paper.

<sup>8</sup> R. F. Soohoo, *Phys. Rev.* **120**, 1978 (1960).

$q$  and  $\omega$ , but if the Fermi velocity  $v_0$  of the electrons is small enough so that  $v_0q \ll |\omega_c - \omega|$  the dielectric constant is only a function of  $\omega$  and is given by

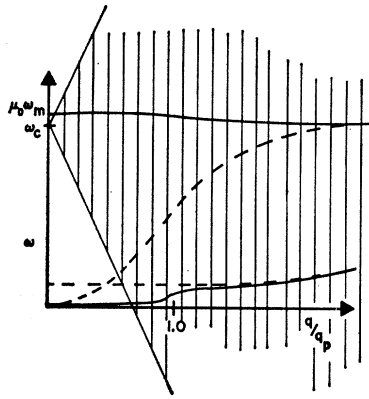
$$\epsilon = 1 - \omega_p^2 / \omega(\omega - \omega_c), \quad (9)$$

where  $\omega_p^2 = 4\pi ne^2/m$ . We will use the convention that  $\omega < 0$  reverses the sense of the circularly polarized wave. For this model and neglecting the 1 in  $\epsilon$ , Eq. (8) has the solutions

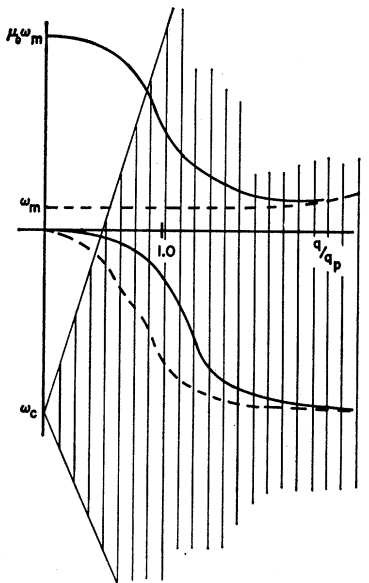
$$\omega = \frac{\omega_h}{2} + \frac{\omega_m}{2} + \frac{2\pi M_s \gamma}{1 + (q/q_p)^2} \pm \left[ \left( \frac{\omega_h}{2} + \frac{\omega_m}{2} + \frac{2\pi M_s \gamma}{1 + (q/q_p)^2} \right)^2 - \omega_m \omega_h \right]^{1/2}, \quad (10)$$

where

$$\begin{aligned} \omega_h &= q^2 \omega_c (q_p^2 + q^2)^{-1}, \\ \omega_c &= eB/mc, \\ q_p^2 &= \omega_p^2 / c^2, \end{aligned}$$



(a)



(b)

FIG. 1. A schematic representation of the helicon and magnon spectra as given in Eq. (10). The spectra in the case of no coupling ( $\mu_0=1$ ) is shown as the dashed curves and the spectra with coupling is shown by the solid curves with  $\mu_0 \approx 8$ . The Doppler-shifted absorption region is represented by the hatched area. Within this hatched area the modes are too highly damped to be observable. Figures 1(a) and 1(b) represent the situation when the conduction electrons are electron-like or hole-like, respectively.

and

$$B = H_0 + 4\pi M_s.$$

Here  $\omega_h$  is the helicon spectrum if there were no coupling with the magnons. To obtain insight, consider the long- and short-wavelength limits,  $q \ll q_p$  and  $q \gg q_p$ , respectively, of Eq. (10).

$$\omega = \mu_0 \omega_m, \quad \omega_h / \mu_0; \quad q \ll q_p, \quad (11)$$

where

$$\mu_0 = 1 + 4\pi M_s \gamma / \omega_m$$

and

$$\omega = \omega_c, \quad \omega_m; \quad q \gg q_p. \quad (12)$$

The two solutions in (11) and (12) correspond to the spin-wave and helicon modes. It is of interest to compare the field distributions for these two types of modes. Consider the case  $q \ll q_p$ . Inserting the two limits given in (11) into Eq. (5) we find that the limit  $\omega = \mu_0 \omega_m$ , the spin-wave mode, corresponds to field distributions of  $H_\phi \approx -4\pi M_\phi$  or  $B_\phi \approx 0$ . The limit  $\omega = \omega_h / \mu_0$ , the helicon mode, corresponds to field distributions of  $(\mu_0 - 1)H_\phi = 4\pi M_\phi$  or  $B_\phi = \mu_0 H_\phi$ . We see that at long wavelengths (but short compared with the sample size) the magnon frequencies are increased by the factor  $\mu_0$ , while the helicon frequencies are decreased by the factor  $\mu_0^{-1}$ . For iron and in zero external field  $\mu_0 \approx 23$  so that the interaction causes a spectacular effect at long wavelengths. The result given in (11) for the helicon mode can be easily understood from Eq. (8') where we see that  $\mu_0$  is just the magnetic permeability of the magnetic spins at low frequencies. At short wavelengths the solutions given in (12) are the same as those for the magnons and helicons without interaction.

Figure 1 gives a schematic plot of (10). The dashed curves are the magnon and helicon spectra if there were no interaction between them. The two possibilities are shown where  $\omega_c / \omega_m > 0$  and  $\omega_c / \omega_m < 0$ . These correspond to the cases of electrons and holes, respectively. In the case where  $(\omega_c / \omega_m) > 0$  the branch for the helicon-like mode at small  $q$  becomes the magnon mode at large  $q$  and vice versa. In the case where  $(\omega_c / \omega_m) < 0$  both the magnon- and helicon-type modes retain their identity for all  $q$ .

The parameter  $(\mu_0 - 1)$  determines the coupling between magnons and helicons. When  $(\mu_0 - 1)$  is large there is a large coupling while when  $\mu_0 - 1 = 0$  there is no coupling. We have already seen how a large  $(\mu_0 - 1)$  produces a large effect for  $q \ll q_p$ . When  $\mu_0 - 1 = 0$ , Eq. (10) has the solutions

$$\omega = \omega_m, \quad \omega_h. \quad (10')$$

The spectra in (10') are the free magnon and helicon spectra, respectively. We see from (10) and (7) that  $\mu_0$  can be varied by changing the external magnetic field. Thus, an experiment can be performed on a magnetic conductor such as iron where it is possible to measure from the strong-coupling limit to the weak-coupling limit by merely varying the external field.

In a real magnetic conductor the model chosen for  $\epsilon$  in (9) has to be modified in three ways. One, the spin-orbit interaction has to be considered; two, the approximation  $v_0q \ll |\omega_c - \omega|$  is only correct for small  $q$ ; and, three, finite relaxation times must be considered.

The spin-orbit interaction, as pointed out by Kittel,<sup>9</sup> does not act like a magnetic field because the spin-orbit potential is periodic, and the time-independent electronic eigenstates are still Bloch waves. Thus, the spin-orbit interaction does not affect the Lorentz force on the electrons in Bloch states of wave vector  $\mathbf{k}$ , and it is still given by

$$\frac{\hbar d\mathbf{k}}{dt} = e \left( \mathbf{E} + \frac{\mathbf{v} \times \mathbf{B}}{c} \right), \quad (13)$$

where  $B$  is given by the same expression as in (10). The spin-orbit interaction does, however, contribute to the dielectric constant through a polarization of the electrons,<sup>10</sup> but it can be shown that this makes a negligible contribution to the dielectric constant at the low frequencies of helicon propagation. On the other hand, at optical frequencies this spin-orbit polarization is the cause of the very large Faraday and Kerr rotations in ferromagnetic metals.<sup>11</sup> We shall elaborate upon this in a subsequent paper.

In real metals the velocity of the electrons at the Fermi surface,  $v_0$ , is such that  $v_0q \ll |\omega_c - \omega|$  is not usually satisfied. The expression in this case for  $\epsilon$  neglecting 1 becomes<sup>12,13</sup>

$$\text{Re}\epsilon = [\omega_p^2 / \omega(\omega_c - \omega)] F(x),$$

where

$$F(x) = \frac{3}{4}x \{ (1-x^2) \ln |(1-x)/(1+x)| - 2x \}, \quad (14)$$

and

$$x = (\omega_c - \omega) / qv_0.$$

$$\text{Im}\epsilon = \frac{3}{4}\pi (\omega_p^2 / \omega qv_0) (1 - x^2), \quad x^2 \leq 1.$$

Here  $\text{Im}$  and  $\text{Re}$  mean imaginary and real parts.

It is seen from (14) that even for  $qv_0 = \omega_c - \omega$  there is no major change in  $\text{Re}\epsilon$  which is only increased by 50% over the simple form in (9). The main change occurs in the  $\text{Im}\epsilon$  which becomes finite for  $qv_0 > |\omega_c - \omega|$ . This means that the magnon and helicon modes will become damped in this region. The physical origin of this damping mechanism can be easily understood. If in the conductor a wave of frequency  $\omega$  and wave number  $q$  is present, then an electron of velocity  $v_0$  experiences, because of the usual Doppler-shift, a frequency

$$\omega' = \omega \pm v_0q. \quad (15)$$

If  $\omega'$  coincides with the cyclotron frequency of the electron  $\omega_c$ , the absorption of the energy of the wave

by the electron will occur at

$$\omega_c - \omega = v_0q. \quad (16)$$

Figure 1 also illustrates the Doppler-shifted damping region and shows schematically the magnon and helicon spectra in that case. In real metals, then, the region for observing the predicted helicon-magnon coupling is appreciably reduced from that of the simple model as represented by (9).

The helicons will be highly damped even for  $qv_0$  slightly greater than  $(\omega_c - \omega)$ . For all greater values of  $q$  the helicon mode is damped so severely that it ceases to exist. This is indicated on Fig. 1 by extending the hatched lines over the entire part of the helicon mode where  $qv_0 > |\omega_c - \omega|$ . The magnon mode is also highly damped for  $qv_0$  slightly greater than  $(\omega_c - \omega)$ . However, this severely damped region does not extend to all values of  $q$ . For very large  $q$  where the  $q$  dependence of  $\omega_m$  becomes dominant the lossy nature of  $\epsilon$  has no longer a damping effect.

Till now the discussion has neglected effects of finite relaxation times. The expressions for  $\epsilon$  given in both (9) and (14) assume that  $|\omega_c - \omega| \tau \gg 1$ . The expression for  $\mu$  given in (8') assumes that  $|\omega_m - \omega| \tau_m \gg 1$ , where  $\tau_m$  is defined as the imaginary part of  $\omega_m$  arising from the lossy terms in the Landau-Lifshitz equation. The effects of these finite relaxation times can be included in the previous work simply by replacing  $\omega_c$  by  $(\omega_c + i/\tau)$  and  $\omega_m$  by  $(\omega_m + i/\tau_m)$ . Thus, for instance, we see that finite relaxation times in Eq. (10) make  $\omega$  complex describing the damping in time of modes which vary in space as  $e^{iqz}$ . This damping is small as long as both  $\omega_c \tau \gg 1$  and  $\omega_m \tau_m \gg 1$ .

The propagation of the modes in space is more severely effected by the finite relaxation times. Considering the problem of the excitation of these modes on a plane  $z = z_0$ , the modes will become highly damped in their propagation through space when either, or both,  $|\omega_c - \omega| \tau < 1$  and  $|\mu_0 \omega_m - \omega| \tau_m < 1$ . Clearly, for any finite  $\tau$  there exists a band of frequencies around  $\omega_c$  where this will occur. This damping is important only in the case of electron conduction illustrated in Fig. 1(a). It may impose a more severe restriction on the perfection of the material for propagation of modes on the upper branch than the lower branch. In order to see the upper branch  $|\mu_0 \omega_m - \omega| \tau > 1$ , whereas in the lower branch it is required that  $\omega_c \tau > 1$ . The effect of a finite relaxation time  $\tau_m$  in  $\mu$  places a particularly severe restriction on the propagation of the modes in the upper branch. This condition appears to be very difficult to satisfy for modes in the upper branch. However, even when this condition is not satisfied, vestiges of this mode will remain, for example, as an anomalously large penetration depth. In any case, the modes of the lower branch easily satisfy this condition and should show the predicted effects. Attenuation of the upper branch modes may prove to be a very sensitive way to measure the Landau-Lifshitz damping in metals.

<sup>9</sup> C. Kittel, Phys. Rev. **108**, 1097 (1957).

<sup>10</sup> J. Smit, Physica **21**, 877 (1955).

<sup>11</sup> P. N. Argyres, Phys. Rev. **97**, 334 (1955).

<sup>12</sup> R. G. Chambers, Phil. Mag. **1**, 459 (1956).

<sup>13</sup> P. B. Miller and K. K. Haering, Phys. Rev. **128**, 126 (1962).

Appreciation of the transmission characteristics of a highly conducting ferromagnetic medium is gained by consideration of the frequency dependence of the dielectric constant and permeability. For simplicity we will consider the case of the local dielectric constant of Eq. (9) rather than the more general Eq. (14) and we ignore damping. According to Eq. (1), propagating solutions will exist only when the product  $\mu\epsilon$  is positive. From Eq. (9), the dielectric constant is positive for frequencies less than  $\omega_c$  and negative for  $\omega > \omega_c$ . Considering for the moment the behavior of  $\mu$  along the  $q=0$  axis, from Eq. (8') we see that  $\mu$  is positive at  $\omega=0$  and rises toward infinity as  $\omega$  approaches  $\omega_m$  from below. Thus, in the region below  $\omega_m$  both  $\epsilon$  and  $\mu$  are positive, and there is a band of frequencies in which the medium is transparent.

At frequencies immediately above  $\omega_m$  the permeability reverses sign to  $-\infty$ , and increases with increasing frequency. Hence, in this region the permeability is negative and the dielectric constant is positive, and there is a reflection band of metallic behavior. There are two possibilities for the upper edge of this reflection band, depending upon the particular values of the  $g$  factor, the anisotropy field, and principally upon the effective mass of the charge carriers (and, hence, upon the direction of propagation). Either  $\omega_c$  lies above or below  $\mu_0\omega_m$ . If  $\omega_c$  lies above  $\mu_0\omega_m$ , then the upper edge of the reflection band is at  $\mu_0\omega_m$  at which frequency  $\mu=0$ . In the region above  $\mu_0\omega_m$  both  $\epsilon$  and  $\mu$  are again greater than zero and transmission occurs. This pass band extends up to  $\omega_c$ , where  $\epsilon$  changes sign. In this case the upper branch starts at  $\mu_0\omega_m$  at  $q=0$  and rises with increasing  $q$  up to  $\omega_c$ . Above  $\omega_c$ ,  $\mu$  is positive, approaching one as  $\omega \rightarrow \infty$ , and  $\epsilon$  is negative, becoming zero at  $\omega \approx \omega_p$ . Thus, no other transmission bands occur below  $\omega_p$ .

If circumstances are such that  $\omega_c < \mu_0\omega_m$ , then  $\omega_c$  determines the upper edge of the intermediate reflection band. In the region between  $\omega_c$  and  $\mu_0\omega_m$ , both  $\epsilon$  and  $\mu$  are negative, and transmission again occurs. The allowed frequencies start at  $\mu_0\omega_m$  at  $q=0$ , and drop to  $\omega_c$  with increasing  $q$ . This is the circumstance depicted in Fig. 1(a).

### III. NUMERICAL ESTIMATE

It is of interest to estimate the magnitude of quantities involved in the helicon-magnon coupling to determine if it can be experimentally observed. We consider the case of iron in no external field which then has the

TABLE I. Estimate of quantities involved in the helicon-magnon coupling in iron.

$4\pi M$	22 000 G
$H_{\text{anis}}$	1000 G
$n$	$10^{23} \text{ cm}^{-3}$
$g$	2.14
$v_0$	$10^8 \text{ cm/sec}$
$\omega_m$	$9.4 \times 10^9 \text{ sec}^{-1}$
$\omega_c$	$3.52 \times 10^{11} \text{ sec}^{-1}$
$\mu_0$	23
$\alpha$	$0.1 \text{ cm}^2 \text{ sec}^{-1}$

properties given in Table I. It is seen from Eq. (10) that the coupling between the helicons and magnons is strongest for

$$q < q_p \approx 6 \times 10^5 \text{ cm}^{-1},$$

which corresponds to wavelengths larger than  $10^{-5} \text{ cm}$ . The Doppler-shifted frequency cutoff condition in (16) gives a value of

$$\begin{aligned} q &\leq (\omega_c - \omega)/v_0 \\ &\approx 3.4 \times 10^2 \text{ cm}^{-1} \text{ for upper branch in Fig. 1(a)} \\ &\approx 3.5 \times 10^3 \text{ cm}^{-1} \text{ for lower branch in Fig. 1(a)} \\ &\approx 7.3 \times 10^3 \text{ cm}^{-1} \text{ for upper branch in Fig. 1(b)} \\ &\approx 3.5 \times 10^3 \text{ cm}^{-1} \text{ for lower branch in Fig. 1(b)}. \end{aligned}$$

We see that the Doppler-shifted absorption is the mechanism restricting the region of observation of the magnon-helicon coupling, but this region is very accessible experimentally. In addition, the  $|\omega_c - \omega|/\tau \gg 1$  condition, of course, must be satisfied which restricts the observation of the effects considered here to very pure materials at very low temperatures. It is appropriate to emphasize that the effects discussed in this paper occur in bulk samples and are not limited to skin depth regions. This is because the material is transparent to the electromagnetic modes described in this paper. Thus, whenever the exciting fields penetrate the material they will not be limited to the ordinary skin depth region but will propagate through the medium being attenuated only by processes described by the imaginary parts of  $\mu$  and  $\epsilon$ .

We caution that our discussion has been limited to the case of propagation along the magnetic field direction. While propagation in other directions is complicated by the tensor nature of the medium, it is easily seen that helicons do not exist for propagation normal to the  $B$  field. Thus, Azbel'-Känér geometry of cyclotron resonance is inappropriate to helicon excitation.